ELSEVIER

International Journal of Mass Spectrometry 182/183 (1999) 121–138

International Journal of Mass Spectrometry

Sigma-bond metathesis reactions of $Sc(OCD_3)_2^+$ with water, ethanol, and 1-propanol: measurements of equilibrium constants, relative bond strengths, and absolute bond strengths

Kevin C. Crellin[a,1], J.L. Beauchamp[a,*], W.A. Goddard III[b], S. Geribaldi[c], M. Decouzon[c]

[a]*Arthur Amos Noyes Laboratory of Chemical Physics, California Institute of Technology, Pasadena, CA 91125, USA*
[b]*Materials and Process Simulations Center, Beckman Institute, 139-74, California Institute of Technology, Pasadena, CA 91125, USA*
[c]*Laboratoire de Chimie Physique Organique, Groupe FT-ICR, Université de Nice-Sophia Antipolis, Faculté des Sciences, Parc Valrose, 06108 Nice Cedex 2, France*

Received 12 October 1998; accepted 20 October 1998

Abstract

Fourier transform ion cyclotron resonance (FTICR) mass spectrometry has been used to examine the reactions of $Sc(OCD_3)_2^+$ with water, ethanol, and 1-propanol. Sigma-bond metathesis resulting in the elimination of CD_3OH is the initial reaction observed, with further solvation of the metal center and subsequent elimination of hydrogen occurring as additional reaction channels. These processes are facile at room temperature and involve little or no activation energy. Measured equilibrium constants for the reaction $Sc(OCD_3)_2^+ + ROH \rightleftharpoons CD_3OScOR^+ + CD_3OH$ with R = H, ethyl, and *n*-propyl are 0.013 ± 0.004, 0.5 ± 0.15, and 0.7 ± 0.2, respectively. For the reaction $ROScOCD_3^+ + ROH \rightleftharpoons Sc(OR)_2^+ + CD_3OH$ with R = H and ethyl the measured equilibrium constants are 0.013 ± 0.004 and 0.3 ± 0.1, respectively. ΔS is estimated for these processes using theoretical calculations and statistical thermodynamics, and in conjunction with the measured equilibrium constants we have evaluated ΔH for these reactions and the relative and absolute bond strengths of the Sc^+–OR bonds, R = H, methyl, ethyl, and *n*-propyl. The relative bond strengths, $D^o_{298}(CD_3OSc^+–OR)–D^o_{298}(CD_3OSc^+–OCD_3)$, for R = H, methyl, ethyl, and *n*-propyl are + 11.9, 0, − 0.1, and − 1.4 kcal mol^{-1}, respectively. The absolute bond strengths for $HOSc^+–OCD_3$, $CD_3OSc^+–OCD_3$, $CD_3OSc^+–OC_2H_5$, $CD_3OSc^+–OCH_2CH_2CH_3$, and $H_5C_2OSc^+–OC_2H_5$ are 115.0, 115.0, 114.9, 113.6, and 114.7 kcal mol^{-1}, respectively. Theoretical calculations with an LAV3P* ECP basis set at the level of localized second-order Møller–Plesset perturbation theory were performed to evaluate ΔS and ΔG for the specific equilibria $Sc(OH)_2^+ + CD_3OH \rightleftharpoons CD_3OScOH + H_2O$, $CD_3OScOH + CD_3OH \rightleftharpoons Sc(OCD_3)_2^+ + H_2O$, and $Sc(OCD_3)_2^+ + C_2H_5OH \rightleftharpoons CD_3OScOC_2H_5^+ + CD_3OH$. The theoretically determined ΔG values agree reasonably well with the experimentally determined ΔG values. In accordance with earlier theoretical predictions, these metathesis reactions are consistent with an allowed four-center mechanism similar to that of a $2_\sigma + 2_\sigma$ cycloaddition. (Int J Mass Spectrom 182/183 (1999) 121–138)

Keywords: $Sc(OCD_3)_2^+$; Water; Ethanol; 1-propanol; FTICR; Equilibrium constants; Bond strengths

1. Introduction

Sigma-bond metathesis has been observed in a variety of transition metal systems [1–7], including scandium-containing systems [8–12]. A mechanism

* Corresponding author.

[1] Current address: Finnigan Corporation, 355 River Oaks Parkway, San Jose, CA 95134-1991.

Dedicated to the memory of Ben Freiser to commemorate his many seminal contributions to mass spectrometry and gas phase ion chemistry.

1387-3806/99/$20.00
PII S1387-3806(98)14250-1

involving a four-center transition state is generally invoked for these metathesis reactions (as shown in Scheme 1 for the reaction of $Sc(CD_3)_2^+$ with *n*-butane), in accord with the prediction of Steigerwald and Goddard [13] that certain organometallic species containing an extremely acidic (in the Lewis sense) metal center should exhibit this kind of reactivity. These sigma-bond metathesis processes have proven to be extremely useful in investigating the ligand exchange behavior of the organometallic complexes studied. For example, Bryndza et al. [1] have used equilibrium data from sigma-bond metathesis reactions to determine the relative metal–ligand sigma-bond strengths for several series of transition metal complexes in solution.

Part of the motivation for our previous studies of the sigma-bond metathesis reactions of $Sc(CD_3)_2^+$ and $CH_3ScCH_2CH_3^+$ with small alkanes in the gas phase [10–12] was the hope that equilibrium for reactions (1) or (2) (R = ethyl, propyl, *n*-butyl or isobutyl; R′ = propyl, *n*-butyl or isobutyl) would be observed

$$CD_3Sc^+–CD_3 + R–H \rightleftharpoons CD_3Sc^+–R + CD_3H \quad (1)$$

$$CH_3Sc^+–CH_2CH_3 + R'–H \rightleftharpoons CH_3Sc^+–R' + CH_3CH_3 \quad (2)$$

When CD_3Sc^+–R or CH_3Sc^+–R′ was isolated, no reactivity with methane or ethane, respectively, was observed. The chemical activation provided by the interaction of methane and ethane with CD_3Sc^+–R or CH_3Sc^+–R′, respectively, is apparently insufficient to overcome the intrinsic barrier to sigma-bond metathesis [10–12]. With larger hydrocarbons the reaction sequences were too complex to facilitate observation of equilibria, and the reaction exothermicities were likely too large to quantify the equilibria with room temperature Fourier transform ion cyclotron resonance (FTICR) measurements.

Although exchange equilibria via sigma-bond metathesis were not quantified with alkyl substituents, we reasoned that it might still be possible to observe such reactivity with other classes of ligands. In particular, work by Azzaro et al. [14] has shown that $Sc(OCH_3)_2^+$ can be generated by reactions (3) and (4).

$$Sc^+ + CH_3OH \rightarrow ScOCH_3^+ + H \quad (3)$$

$$ScOCH_3^+ + CH_3OH \rightarrow Sc(OCH_3)_2^+ + H \quad (4)$$

One can surmise that $Sc(OCH_3)_2^+$ might undergo exchange reactions with other alcohols analogous to the reactions seen between $Sc(CH_3)_2^+$ and small alkanes. In this article we extend our previous work with scandium alkyl systems to scandium alkoxide systems and present evidence for observation of ligand exchange equilibria via sigma-bond metathesis between $Sc(OCH_3)_2^+$ and ROH (R = H, ethyl, or *n*-propyl) or $ROScOCH_3^+$ and ROH (R = H or ethyl). We use the measured equilibrium constants to evaluate the relative and absolute bond strengths of these various alkoxide ligands to Sc^+.

2. Experimental

Reactions were investigated with FTICR spectrometry, of which a number of reviews are available [15,16]. Only details relevant to these experiments are outlined here. In the Caltech instrument, a 1-in. cubic trapping cell is located between the poles of a Varian 15-in. electromagnet maintained at 1.0 T. Data collection is accomplished with an IonSpec Omega 386 FTICR data system and associated electronics. Neutral gases are introduced into the cell by separate leak valves, and their pressures are measured with a Schultz–Phelps ion gauge calibrated against an MKS 390 HA-00001SP05 capacitance manometer. The instrument at the University of Nice-Sophia Antipolis also uses a 15-in. electromagnet, but data collection is accomplished with a Bruker data system and associated electronics and pressures are measured with a Bayard–Alpert (BA) ionization gauge (Alcatel BN 111). The operation of the BA gauge has been described previously [14]. Uncertainties in absolute pressures are estimated to be ± 20%. CD_3OH was obtained commercially from Merck Sharp and Dohme, whereas ethanol and 1-propanol were obtained from Aldrich. The purity of all alcohols was

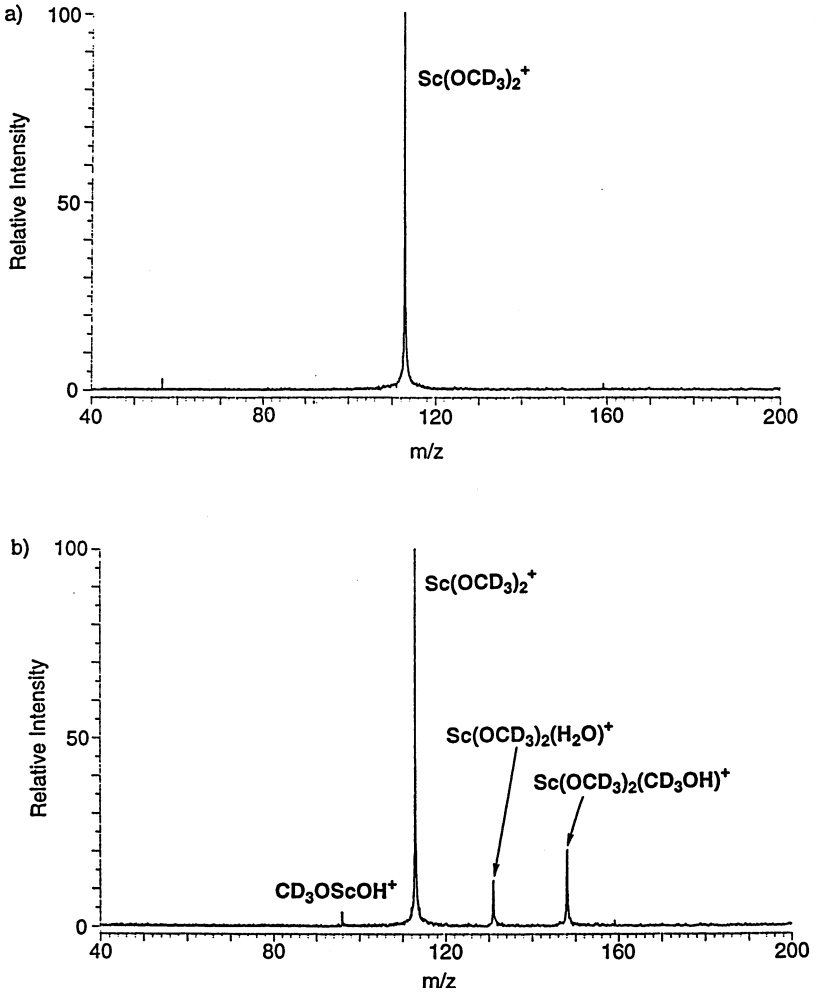

Fig. 1. Reaction of $Sc(OCD_3)_2^+$ with a H_2O/CD_3OH mixture. The pressures of CD_3OH and H_2O were 0.41×10^{-7} Torr and 1.12×10^{-7} Torr, respectively: (a) isolation of $Sc(OCD_3)_2^+$ at $t = 0$ ms, and (b) products of the reaction of $Sc(OCD_3)_2^+$ with the H_2O/CD_3OH mixture. Spectrum taken 700 ms after isolation of $Sc(OCD_3)_2^+$.

99 + %, and the isotopic purity of CD_3OH was 99 + %. All alcohols used were purified by freeze–pump–thaw cycling.

Sc^+ ions were produced by laser ablation of a scandium metal target with an N_2 laser at 337.1 nm [10–12,14]. The reactant ion $Sc(OCD_3)_2^+$ was generated by reaction of Sc^+ with CD_3OH as shown in reactions (3) and (4), and unwanted ions were ejected from the cell using double resonance techniques [17] and/or frequency sweep excitation [18]. Water, ethanol, or 1-propanol was then added along with the labeled methanol and the resulting metathesis reactions were observed. By isolating the resultant CD_3OScOR^+ (R = H, or ethyl) that formed, we were also able to observe a second metathesis reaction. The CD_3OH pressures used in these experiments were in the range $(0.3–1.5) \times 10^{-7}$ Torr, whereas the pressure of the additional alcohols were typically in the range $(0.1–2.0) \times 10^{-7}$ Torr. The H_2O pressures used were in the range $(1.5–2.5) \times 10^{-7}$ Torr. Time plots of the relative abundance of ions versus time were recorded for all reactions. Equilibrium was deemed to have been achieved when the relative ion abundances (with respect to each other) of the two

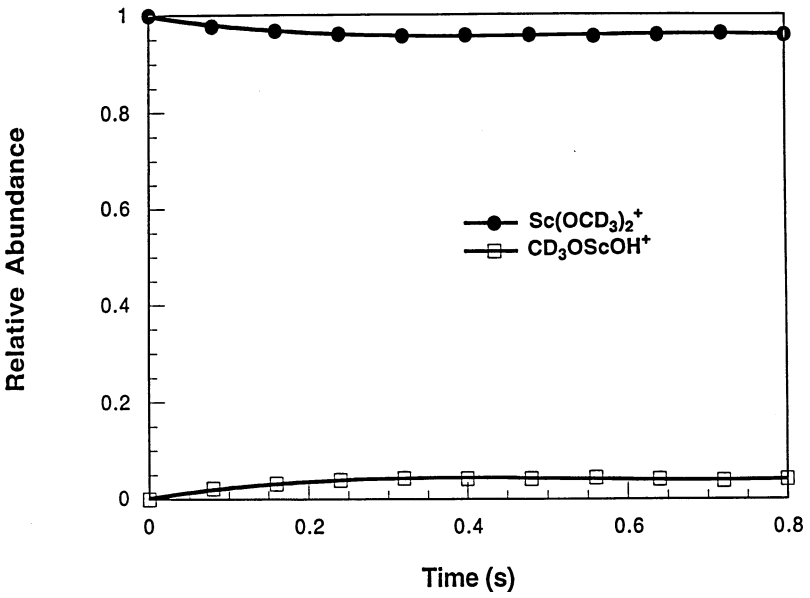

Fig. 2. Time plot of the relative abundance of $Sc(OCD_3)_2^+$ and CD_3OScOH^+ versus time. During this time plot the pressures of CD_3OH and H_2O were 0.47×10^{-7} Torr and 1.43×10^{-7} Torr, respectively. For this specific time plot we find that $K = 0.014$.

ions of interest ceased to vary with time. For the general process $A^+ + B \rightarrow C^+ + D$ the equilibrium constant is derived from Eq. 5, where I_{A^+} and I_{C^+} are the relative intensities of A^+ and C^+ and P_B and P_D are the partial pressures of B and D

$$K = \frac{(I_{C^+})(P_D)}{(I_{A^+})(P_B)} \quad (5)$$

The reported equilibrium constants are averages of several different sets of experimental data taken at different pressures of the neutral gases. Rate constants were calculated from appropriate semilog plots of reactant ion abundance versus time. Where necessary, the systems were modeled by rate expressions for reversible and concurrent reactions to allow us to deconvolute the data [19]. Errors in the rate constants are estimated to be $\pm$ 20% because of uncertainties in the determination of absolute pressure. All experiments were performed at temperatures between 298–303 K.

All the alcohols used in these experiments were unlabeled except for methanol, which was deuterated at the methyl positions (CD_3OH). CD_3OH was used to allow us to distinguish between $Sc(OCH_3)_2^+$ and $HOScOCH_2CH_3^+$, which would otherwise have identical masses. Because the observed sigma-bond metathesis reactions occur at the oxygen atom in alcohols, the labeling in CD_3OH should not give rise to kinetic isotope effects. The labeling has a small secondary isotope effect on the O–H bond strength in CD_3OH ($D^o_{298}[CD_3O–H] = 104.2$ kcal mol^{-1} [20], whereas $D^o_{298}[CH_3O–H] = 104.4$ kcal mol^{-1} [21]), and we presume that the secondary isotope effect on the Sc^+–OCD_3 bond strength in CD_3OScOR^+ would be similar.

3. Results

3.1. Reaction of $Sc(OCD_3)_2^+$ with water

The processes of interest to us are the metathesis reactions (6) and (7)

$$Sc(OCD_3)_2^+ + H_2O \rightleftharpoons CD_3OScOH^+ + CD_3OH \quad (6)$$

$$CD_3OScOH^+ + H_2O \rightleftharpoons Sc(OH)_2^+ + CD_3OH \quad (7)$$

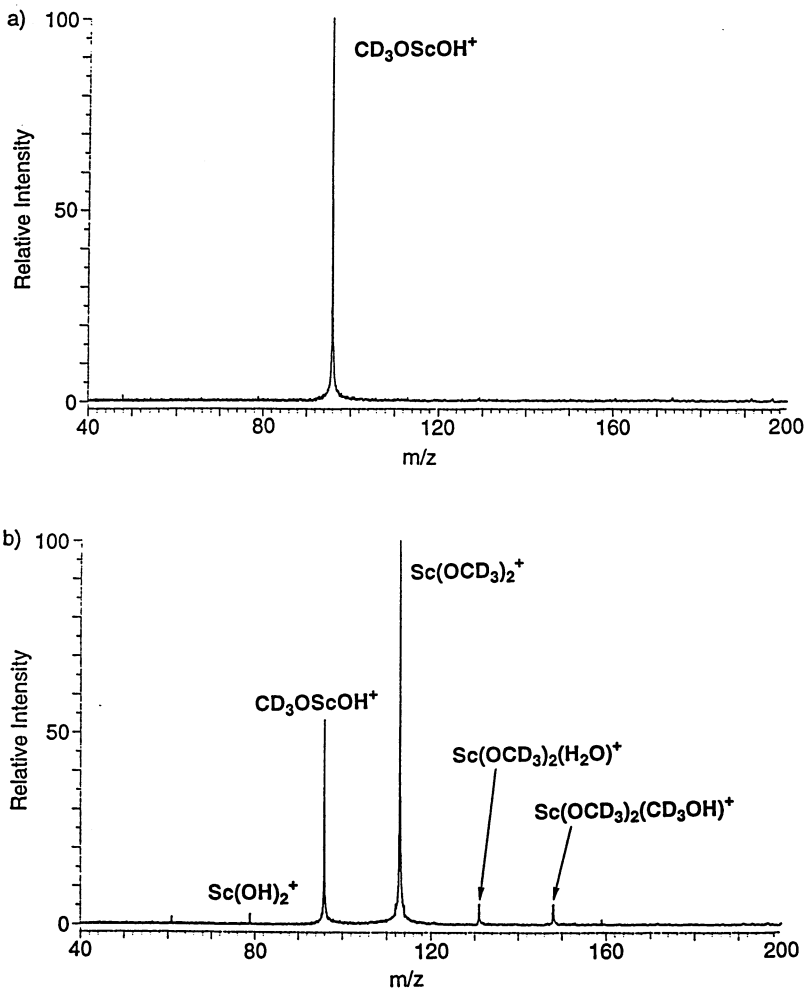

Fig. 3. Reaction of CD_3OScOH^+ with a H_2O/CD_3OH mixture. The pressures of CD_3OH and H_2O were 0.45×10^{-7} Torr and 1.43×10^{-7} Torr, respectively: (a) isolation of CD_3OScOH^+ at $t = 0$ ms, and (b) products of the reaction of CD_3OScOH^+ with the H_2O/CD_3OH mixture. Spectrum taken 450 ms after isolation of CD_3OScOH^+.

However, in addition to these metathesis processes, several solvation processes [reactions (8)–(10)] are also observed. Higher mass clusters were not seen

$$Sc(OCD_3)_2^+ + H_2O \rightarrow Sc(OCD_3)_2(H_2O)^+ \quad (8)$$

$$Sc(OCD_3)_2^+ + CD_3OH \rightarrow Sc(OCD_3)_2(CD_3OH)^+ \quad (9)$$

$$CD_3OScOH^+ + CD_3OH \rightarrow CD_3OScOH(CD_3OH)^+ \quad (10)$$

Equilibrium was established for reactions (6) and (7). In some experiments $Sc(OCD_3)_2^+$ was isolated [see Fig. 1(a)] and allowed to react with water. A typical mass spectrum of the products is shown in Fig. 1(b). In Fig. 2 we present a time plot of the relative abundance of $Sc(OCD_3)_2^+$ and CD_3OScOH^+ versus time. For $Sc(OCD_3)_2^+$ we found that the rate constants for solvation with water and CD_3OH, k_8 and k_9, are 1.7×10^{-11} and 6.2×10^{-11} $cm^3\ s^{-1}\ mol^{-1}$, respectively. For reaction (6) we find that the equilibrium constant K is 0.013. With this value of K we can calculate that the forward and reverse rate constants of reaction (6), k_6 and k_{-6}, are 2.9×10^{-11} and 2.0×10^{-9} $cm^3\ s^{-1}\ mol^{-1}$, respectively.

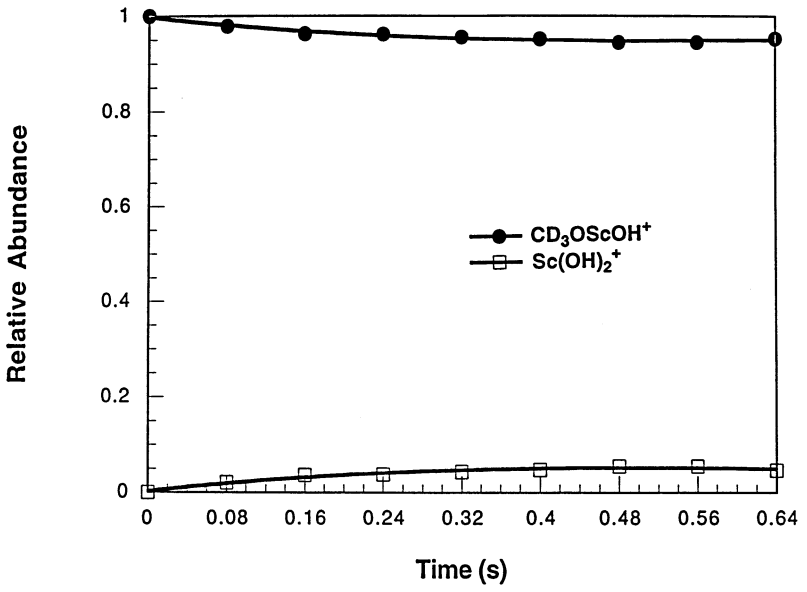

Fig. 4. Time plot of the relative abundance of CD_3OScOH^+ and $Sc(OH)_2^+$ vs. time. During this time plot the pressures of CD_3OH and H_2O were 0.45×10^{-7} Torr and 1.43×10^{-7} Torr, respectively. For this specific time plot we find that $K = 0.013$.

By monitoring the reaction of isolated CD_3OScOH^+ [see Fig. 3(a)] with water [a typical mass spectrum of the products is shown in Fig. 3(b)], we were able to derive time plots of the relative abundance of CD_3OScOH^+ and $Sc(OH)_2^+$ (see Fig. 4). For CD_3OScOH^+ we find that the rate constant of metathesis with CD_3OH, k_{-6}, is 1.7×10^{-9} cm^3 s^{-1} mol^{-1}, in good agreement with the value derived from the reaction of $Sc(OCD_3)_2^+$ with water. For reaction (7) we find that the equilibrium constant K is 0.013. With this value of K we can calculate that the forward and reverse rate constants of reaction (7), k_7 and k_{-7}, are 3.3×10^{-11} and 2.3×10^{-9} cm^3 s^{-1} mol^{-1}, respectively.

Reaction (6) reaches equilibrium quickly and the half life to reach equilibrium is 0.22 s, whereas the half life for the solvation of $Sc(OCD_3)_2^+$ with methanol is 8.5 s. This suggests that the equilibrium constant derived was not effected by the solvation of $Sc(OCD_3)_2^+$. For CD_3OScOH^+, the rate constant of metathesis with CD_3OH, k_{-6}, is only slightly smaller than the reverse rate constant, k_{-7}, of reaction (7); and the half life for reaction (7) to reach equilibrium is 0.19 s, whereas the half life for metathesis with CD_3OH is 0.18 s. However, reaction (7) usually reached equilibrium, whereas the relative intensity of CD_3OScOH^+ was greater than 80%. Thus, although it is possible that the observed equilibrium constant was adversely effected by the metathesis reaction of CD_3OScOH^+ with CD_3OH, we believe that the observed equilibrium constant for reaction (7) is near its true value.

3.2. Reaction of $Sc(OCD_3)_2^+$ with ethanol

The processes of interest to us are the metathesis reactions (11) and (12)

$$Sc(OCD_3)_2^+ + CH_3CH_2OH \rightleftharpoons CD_3OScOCH_2CH_3^+ + CD_3OH \quad (11)$$

$$CD_3OScOCH_2CH_3^+ + CH_3CH_2OH \rightleftharpoons Sc(OCH_2CH_3)_2^+ + CD_3OH \quad (12)$$

In addition to these metathesis processes several solvation [reactions (9) and (13)–(18)] and elimination [reactions (19)–(21)] processes are also observed

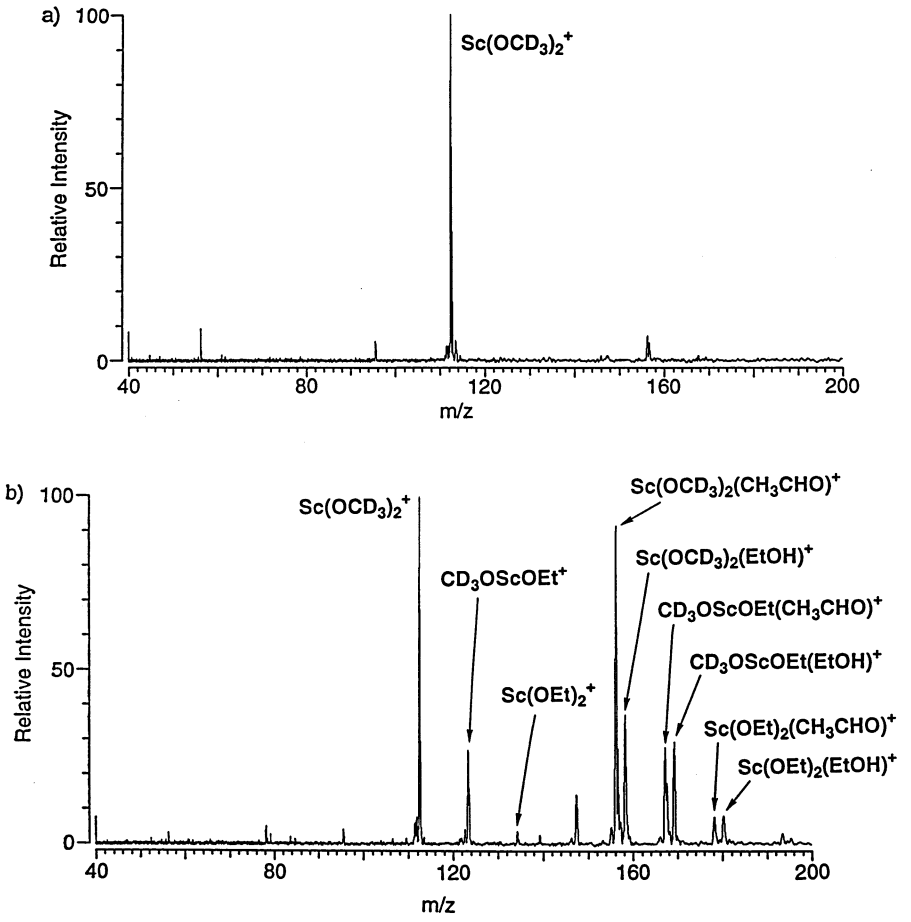

Fig. 5. Reaction of $Sc(OCD_3)_2^+$ with a CD_3OH/CH_3CH_2OH mixture. The pressures of CD_3OH and CH_3CH_2OH were 1.16×10^{-7} Torr and 0.71×10^{-7} Torr, respectively: (a) isolation of $Sc(OCD_3)_2^+$ at $t = 0$ ms, and (b) products of the reaction of $Sc(OCD_3)_2^+$ with the CD_3OH/CH_3CH_2OH mixture. Spectrum taken 400 ms after isolation of $Sc(OCD_3)_2^+$. CH_3CH_2 is abbreviated as Et in this figure. The peaks at m/z 148 and m/z 196 correspond to $Sc(OCD_3)_2(CD_3OH)^+$ and $Sc(OCD_3)_2(CD_3OH)(CH_3CH_2OH)^+$, respectively. We should note that $CD_3OScOCH_2CH_3(CH_3CH_2OH)^+$ and $Sc(OCD_3)_2(CH_3CH_2OH)^+$ could also be $Sc(OCH_2CH_3)_2(CD_3OH)^+$ and $CD_3OScOCH_2CH_3(CD_3OH)^+$, respectively. However, since the reactant ion is $Sc(OCD_3)_2^+$, it is likely that the two former structures are the dominant forms present.

$$Sc(OCD_3)_2^+ + CH_3CH_2OH \rightarrow Sc(OCD_3)_2(CH_3CH_2OH)^+ \quad (13)$$

$$Sc(OCD_3)_2^+ + CD_3OH + CH_3CH_2OH \rightarrow Sc(OCD_3)_2(CD_3OH)(CH_3CH_2OH)^+ \quad (14)$$

$$CD_3OScOCH_2CH_3^+ + CD_3OH \rightarrow CD_3OScOCH_2CH_3(CD_3OH)^+ \quad (15)$$

$$CD_3OScOCH_2CH_3^+ + CH_3CH_2OH \rightarrow CD_3OScOCH_2CH_3(CH_3CH_2OH)^+ \quad (16)$$

$$Sc(OCH_2CH_3)_2^+ + CD_3OH \rightarrow Sc(OCH_2CH_3)_2(CD_3OH)^+ \quad (17)$$

$$Sc(OCH_2CH_3)_2^+ + CH_3CH_2OH \rightarrow Sc(OCH_2CH_3)_2(CH_3CH_2OH)^+ \quad (18)$$

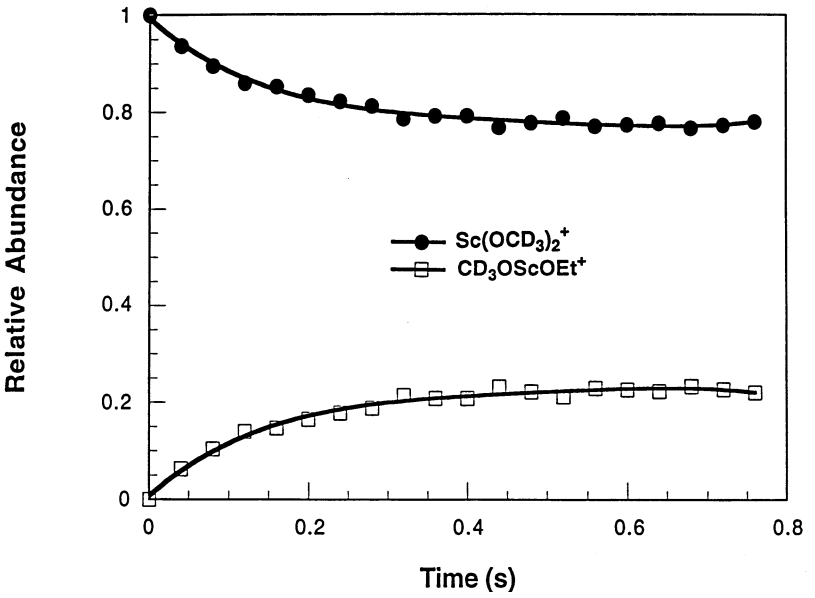

Fig. 6. Time plot of the relative abundance of $Sc(OCD_3)_2^+$ and $CD_3OScOCH_2CH_3^+$ vs. time. CH_3CH_2 is abbreviated as Et in this figure. During this time plot the pressures of CD_3OH and CH_3CH_2OH were 1.16×10^{-7} Torr and 0.71×10^{-7} Torr, respectively. For this specific time plot we find that $K = 0.46$.

$$Sc(OCD_3)_2^+ + CH_3CH_2OH \rightarrow Sc(OCD_3)_2(CH_3CHO)^+ + H_2 \quad (19)$$

$$CD_3OScOCH_2CH_3^+ + CH_3CH_2OH \rightarrow CD_3OScOCH_2CH_3(CH_3CHO)^+ + H_2 \quad (20)$$

$$Sc(OCH_2CH_3)_2^+ + CH_3CH_2OH \rightarrow Sc(OCH_2CH_3)_2(CH_3CHO)^+ + H_2 \quad (21)$$

We did not attempt to observe higher mass clusters. No HD loss is seen, indicating that the elimination of hydrogen from complexed methanol does not occur. Such clustering has been observed previously between $Sc(OCH_3)_2^+$ and CH_3OH [14]. Equilibrium was established for reactions (11) and (12). In some experiments $Sc(OCD_3)_2^+$ was isolated [see Fig. 5(a)] and allowed to react with ethanol. A typical mass spectrum of the products is shown in Fig. 5(b). In Fig. 6 we show a time plot of the relative abundance of $Sc(OCD_3)_2^+$ and $CD_3OScOCH_2CH_3^+$ versus time. For $Sc(OCD_3)_2^+$ we found that the rate constants of solvation with CD_3OH and CH_3CH_2OH, k_9 and k_{13}, are 6.1×10^{-11} and 7.7×10^{-10} cm^3 s^{-1} mol^{-1}, respectively. The value of k_9 derived here is in excellent agreement with the value derived when $Sc(OCD_3)_2^+$ is reacted with CD_3OH/water mixtures. For reaction (11) we find that the equilibrium constant K is 0.5. With this value of K we can calculate that the forward and reverse rate constants of reaction (11), k_{11} and k_{-11}, are 4.6×10^{-10} and 9.3×10^{-10} cm^3 s^{-1} mol^{-1}, respectively.

By monitoring the reaction of the isolated $CD_3OScOCH_2CH_3^+$ [see Fig. 7(a)] with ethanol [a typical mass spectrum of the products is shown in Fig. 7(b)], we were also able to derive time plots of the relative abundance of $CD_3OScOCH_2CH_3^+$ and $Sc(OCH_2CH_3)_2^+$ (see Fig. 8). For $CD_3OScOCH_2CH_3^+$ we find that the rate constants of solvation with CD_3OH and CH_3CH_2OH, k_{15} and k_{16}, are 5.4×10^{-10} and 4.1×10^{-10} cm^3 s^{-1} mol^{-1}, respectively. For $CD_3OScOCH_2CH_3^+$ we find that the rate constant of metathesis with CD_3OH, k_{-11}, is 7.2×10^{-10} cm^3 s^{-1} mol^{-1}, in reasonable agreement with the value derived from the reaction of $Sc(OCD_3)_2^+$ with ethanol.

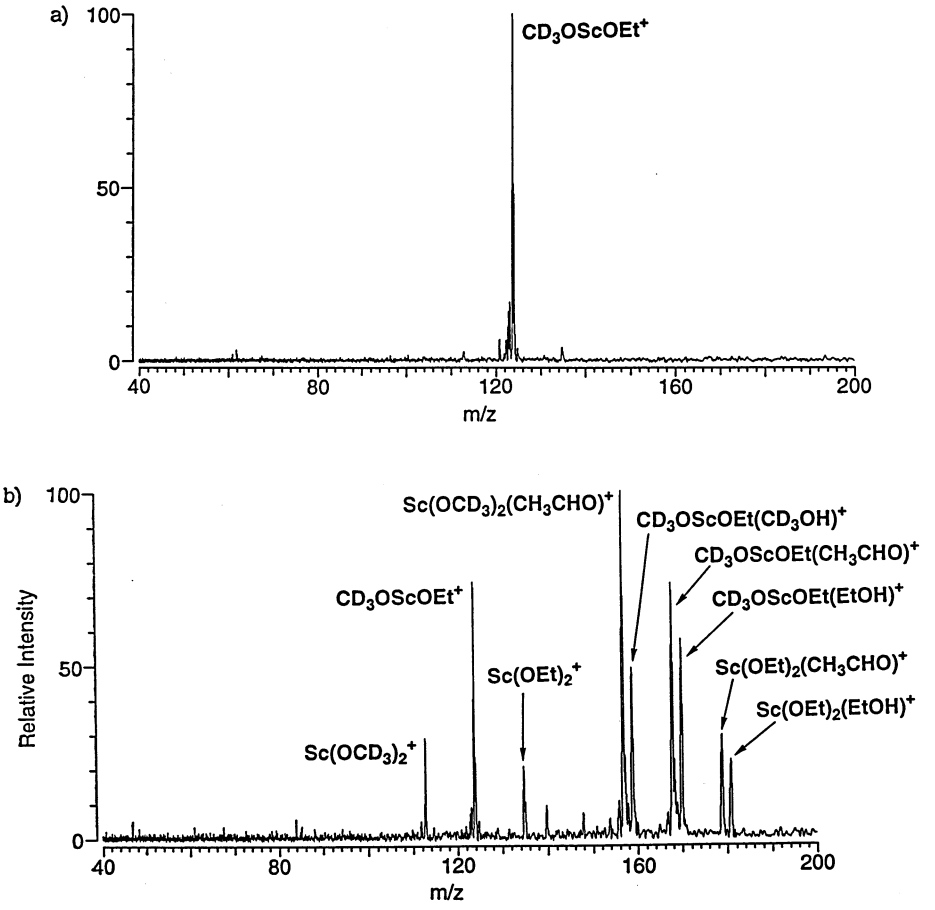

Fig. 7. Reaction of $CD_3OScOCH_2CH_3^+$ with a CD_3OH/CH_3CH_2OH mixture. The pressures of CD_3OH and CH_3CH_2OH were 0.69×10^{-7} Torr and 0.75×10^{-7} Torr, respectively. CH_3CH_2 is abbreviated as Et in this figure: (a) isolation of $CD_3OScOCH_2CH_3^+$ at $t = 0$ ms, and (b) products of the reaction of $CD_3OScOCH_2CH_3^+$ with the CD_3OH/CH_3CH_2OH mixture. Spectrum taken 540 ms after isolation of $CD_3OScOCH_2CH_3^+$. Note that $CD_3OScOCH_2CH_3(CD_3OH)^+$ and $CD_3OScOCH_2CH_3(CH_3CH_2OH)^+$ could also be $Sc(OCD_3)_2(CH_3CH_2OH)^+$ and $Sc(OCH_2CH_3)_2(CD_3OH)^+$, respectively. However, since the reactant ion is $CD_3OScOCH_2CH_3^+$, it is likely that the two former structures are the dominant forms present.

For reaction (12) we find that the equilibrium constant K is 0.3. With this value of K we can calculate that the forward and reverse rate constants of reaction (12), k_{12} and k_{-12}, are 2.3×10^{-11} and 7.5×10^{-10} cm^3 s^{-1} mol^{-1}, respectively.

For reaction (11), equilibrium is usually reached when the relative intensity of $Sc(OCD_3)_2^+$ is greater than 80%. Furthermore, the half life to reach equilibrium is 0.12 s, whereas the half life for the solvation of $Sc(OCD_3)_2^+$ with ethanol is 0.39 s. This suggests that the observed equilibrium constant is not effected by the solvation of $Sc(OCD_3)_2^+$. For $CD_3OScOCH_2CH_3^+$, the rate constants for solvation with CD_3OH and CH_3CH_2OH, k_{15} and k_{16}, are comparable to the reverse rate constant of reaction (12). However, even though the half life to reach equilibrium is 0.31 s whereas the half life for the solvation of $CD_3OScOCH_2CH_3^+$ with methanol is 0.58 s, equilibrium was generally not reached until the relative intensity of $CD_3OScOCH_2CH_3^+$ had fallen below 50%. Thus it is possible that the observed equilibrium constant for reaction (12) was adversely effected by the competing solvation processes.

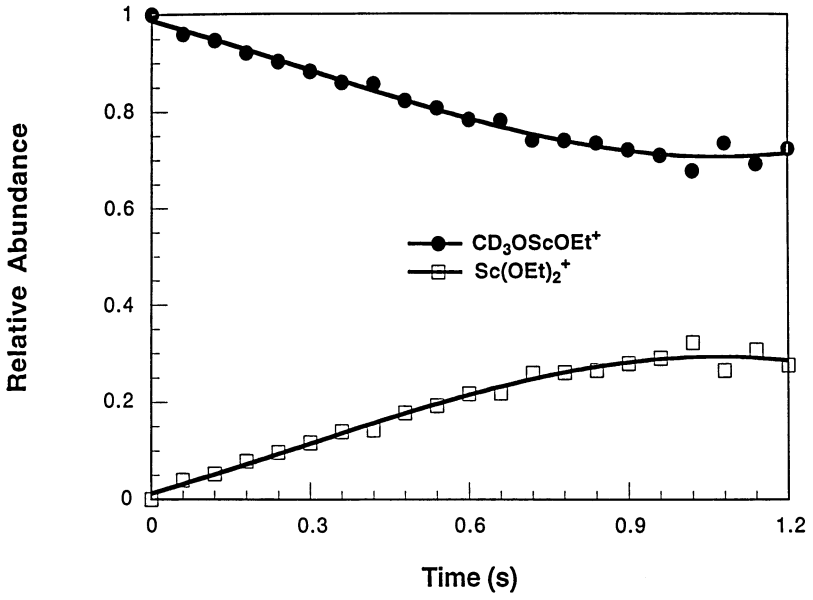

Fig. 8. Time plot of the relative abundance of $CD_3OScOCH_2CH_3^+$ and $Sc(OCH_2CH_3)_2^+$ vs. time. CH_3CH_2 is abbreviated as Et in this figure. During this time plot the pressures of CD_3OH and CH_3CH_2OH were 0.69×10^{-7} Torr and 0.75×10^{-7} Torr, respectively. For this specific time plot we find that $K = 0.38$.

3.3. Reaction of $Sc(OCD_3)_2^+$ with 1-propanol

The main process of interest to us is the metathesis reaction (22)

$$Sc(OCD_3)_2^+ + CH_3(CH_2)_2OH \rightleftharpoons CD_3OScO(CH_2)_2CH_3^+ + CD_3OH \quad (22)$$

Unfortunately, we were unable to reproducibly measure an equilibrium constant for the reaction of $CD_3OScO(CH_2)_2CH_3^+$ with $CH_3(CH_2)_2OH$ (the half life of this equilibration was considerably slower than the half life of solvation). Again, in addition to reaction (22), several solvation [reactions (9) and (23)–(25)] and elimination [reactions (26) and (27)] processes are also observed

$$Sc(OCD_3)_2^+ + CH_3(CH_2)_2OH \rightarrow Sc(OCD_3)_2(CH_3(CH_2)_2OH)^+ \quad (23)$$

$$CD_3OScO(CH_2)_2CH_3^+ + CD_3OH \rightarrow CD_3OScO(CH_2)_2CH_3(CD_3OH)^+ \quad (24)$$

$$CD_3OScO(CH_2)_2CH_3^+ + CH_3(CH_2)_2OH \rightarrow CD_3OScO(CH_2)_2CH_3(CH_3(CH_2)_2OH)^+ \quad (25)$$

$$Sc(OCD_3)_2^+ + CH_3(CH_2)_2OH \rightarrow Sc(OCD_3)_2(CH_3CH_2CHO)^+ + H_2 \quad (26)$$

$$CD_3OScO(CH_2)_2CH_3^+ + CH_3(CH_2)_2OH \rightarrow CD_3OScO(CH_2)_2CH_3(CH_3CH_2CHO)^+ + H_2 \quad (27)$$

We did not attempt to observe higher mass clusters. Equilibrium was established for reaction (22). $Sc(OCD_3)_2^+$ was isolated as shown in Fig. 9(a) and allowed to react with 1-propanol. A typical mass spectrum of the products is shown in Fig. 9(b) and a time plot of the relative abundance of $Sc(OCD_3)_2^+$ and $CD_3OScO(CH_2)_2CH_3^+$ versus time is presented in Fig. 10. We found that the rate constants of solvation with CD_3OH and $CH_3(CH_2)_2OH$, k_9 and k_{23}, are 6.3×10^{-11} and 1.3×10^{-9} $cm^3\ s^{-1}\ mol^{-1}$, respectively. Again, the value of k_9 derived here is in excellent agreement with the value derived when $Sc(OCD_3)_2^+$ is

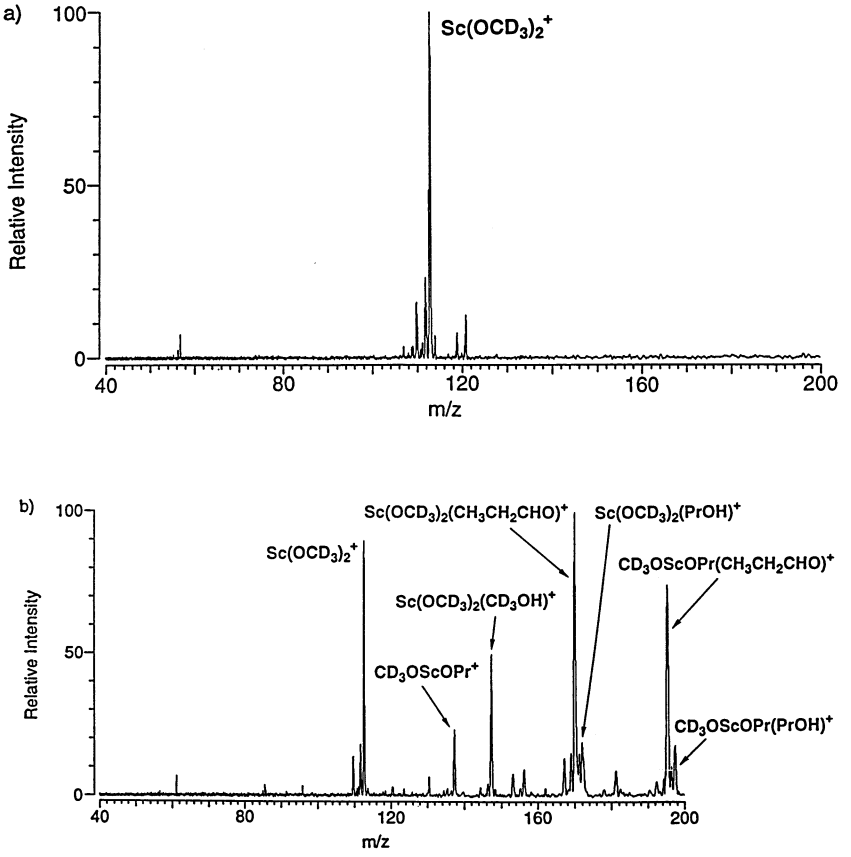

Fig. 9. Reaction of $Sc(OCD_3)_2^+$ with a $CD_3OH/CH_3(CH_2)_2OH$ mixture. The pressures of CD_3OH and $CH_3(CH_2)_2OH$ were 0.58×10^{-7} Torr and 0.14×10^{-7} Torr, respectively: (a) isolation of $Sc(OCD_3)_2^+$ at $t = 0$ ms, and (b) products of the reaction of $Sc(OCD_3)_2^+$ with $CH_3(CH_2)_2OH$. Spectrum taken 1200 ms after isolation of $Sc(OCD_3)_2^+$. $CH_3(CH_2)_2$ is abbreviated as Pr in this figure. We should note that $Sc(OCD_3)_2(CH_3(CH_2)_2OH)^+$ and $CD_3OScO(CH_2)_2CH_3(CH_3(CH_2)_2OH)^+$ could also be $CD_3OScO(CH_2)_2CH_3(CD_3OH)^+$ and $Sc(O(CH_2)_2CH_3)_2(CD_3OH)^+$, respectively. However, since the reactant ion is $Sc(OCD_3)_2^+$, it is likely that the two former structures are the dominant forms present.

reacted with CD_3OH/water mixtures. For reaction (22) we find that the equilibrium constant K is 0.7. With this value of K we can calculate that the forward and reverse rate constants of reaction (22), k_{22} and k_{-22}, are 8.2×10^{-10} and 1.2×10^{-9} cm^3 s^{-1} mol^{-1}, respectively. For reaction (22) the half life to reach equilibrium is 0.27 s, whereas the half life for the solvation of $Sc(OCD_3)_2^+$ with 1-propanol is 1.2 s. Furthermore, the relative intensity of $Sc(OCD_3)_2^+$ is usually greater than 90% when equilibrium is reached. This suggests that the equilibrium constant derived was not effected by the solvation of $Sc(OCD_3)_2^+$. Table 1 presents a summary of the metathesis equilibria we observed.

4. Ab initio calculations

Equilibrium measurements will provide us with ΔG for a reaction, but we cannot calculate ΔH without knowing ΔS. In order to estimate ΔS for these reactions and compare the theoretical values of ΔG to our experimental measurements, we performed ab initio calculations to theoretically evaluate ΔS and ΔH for the metathesis reactions shown in reactions (28), (29), and (30) [identical to the reverse of reaction (7), the reverse of reaction (6), and reaction (11), respectively, except that the methoxide ligands contain H instead of D]

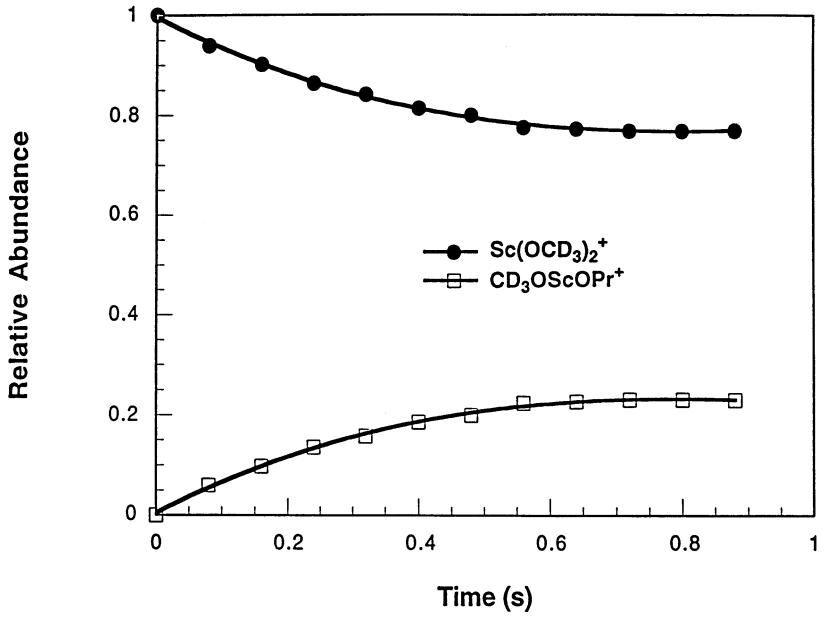

Fig. 10. Time plot of the relative abundance of $Sc(OCD_3)_2^+$ and $CD_3OScOCH_2CH_2CH_3^+$ vs. time. $CH_3CH_2CH_2$ is abbreviated as Pr in this figure. During this time plot the pressures of CD_3OH and $CH_3CH_2CH_2OH$ were 0.58×10^{-7} Torr and 0.23×10^{-7} Torr, respectively. For this specific time plot we find that $K = 0.75$.

$$Sc(OH)_2^+ + CH_3OH \rightleftharpoons CH_3OScOH^+ + H_2O \quad (28)$$

$$CH_3OScOH^+ + CH_3OH \rightleftharpoons Sc(OCH_3)_2^+ + H_2O \quad (29)$$

$$Sc(OCH_3)_2^+ + CH_3CH_2OH \rightleftharpoons CH_3OScOCH_2CH_3^+ + CH_3OH \quad (30)$$

The PS-GVB system of programs [22] was used for all the calculations performed. A 6-31G* basis set was used for C, H and O, whereas for Sc^+ we used an effective core potential (ECP) to replace all but the valence electrons [23]. Initial geometry optimizations were performed at the Hartree–Fock (HF) level for $Sc(OH)_2^+$, CH_3OScOH^+, $Sc(OCH_3)_2^+$, $CH_3OScOCH_2CH_3^+$, H_2O, CH_3OH, and CH_3CH_2OH. These structures were then further optimized at the localized second-order Møller–Plesset (LMP2) perturbation level of theory. Harmonic vibrational frequencies were also calculated

Table 1
Summary of observed ligand exchange equilibria established via sigma-bond metathesis[a]

Process	K	ΔG (kcal mol^{-1})	ΔH (kcal mol^{-1})[b]
$Sc(OH)_2^+ + CD_3OH \rightleftharpoons CD_3OScOH^+ + H_2O$	77 (27)	−2.6 (0.2)	−2.9 (0.6)[c]
$CD_3OScOH^+ + CD_3OH \rightleftharpoons Sc(OCD_3)_2^+ + H_2O$	77 (27)	−2.6 (0.2)	−2.9 (0.6)[c]
$Sc(OCD_3)_2^+ + CH_3CH_2OH \rightleftharpoons CD_3OScOCH_2CH_3^+ + CD_3OH$	0.5 (0.15)	+0.4 (0.1)	+0.1 (0.6)[c]
$CD_3OScOCH_2CH_3^+ + CH_3CH_2OH \rightleftharpoons Sc(OCH_2CH_3)_2^+ + CD_3OH$	0.3 (0.1)	+0.7 (0.2)	+0.3 (0.6)[d]
$Sc(OCD_3)_2^+ + CH_3(CH_2)_2OH \rightleftharpoons CD_3OScO(CH_2)_2CH_3^+ + CD_3OH$	0.7 (0.2)	+0.2 (0.1)	+0.6 (0.6)[e]

[a] Uncertainties are in parenthesis.
[b] All values calculated assuming ambient $T = 298$ K.
[c] Calculated using theoretical LMP2 value of ΔS (see Table 3).
[d] Calculated assuming $\Delta S = -R \ln 2 = -1.38$ cal mol^{-1} K^{-1} [ΔS estimated with Eq. (33)].
[e] Calculated assuming $\Delta S = R \ln 2 = 1.38$ cal mol^{-1} K^{-1} [ΔS estimated with Eq. (33)].

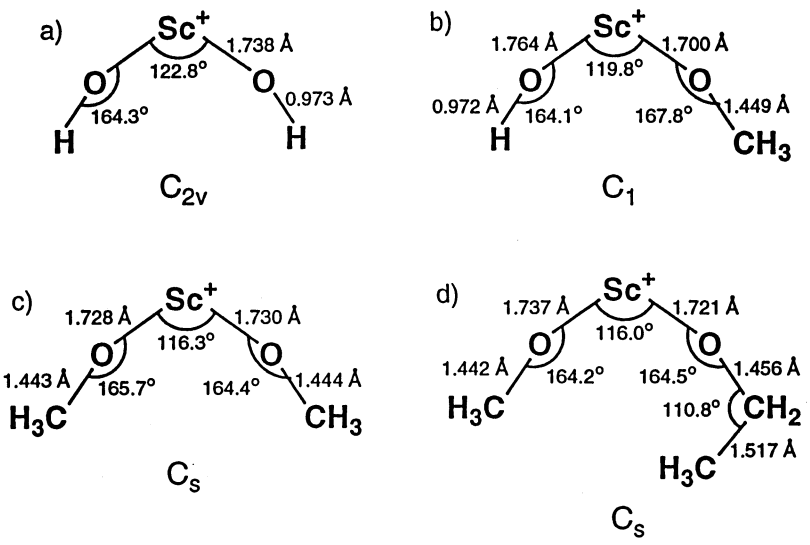

Fig. 11. LMP2 optimized lowest energy geometry for (a) $Sc(OH)_2^+$, (b) CH_3OScOH^+, (c) $Sc(OCH_3)_2^+$, and (d) $CH_3OScOCH_2CH_3^+$. All were calculated using the LAV3P* ECP basis set with no symmetry constraints. The optimized CH_3OScOH^+ and $Sc(OCH_3)_2^+$ geometries deviated slightly from C_S and C_{2v} symmetry, respectively.

for each of these species at the LMP2 level to obtain zero-point energies and absolute entropies at 298 K.

Several different conformations were calculated for $Sc(OH)_2^+$, CH_3OScOH^+, $Sc(OCH_3)_2^+$, and $CH_3OScOCH_2CH_3^+$. Fig. 11 shows the LMP2 optimized lowest energy geometry for these species [24]. Table 2 presents the total energy, zero-point energy, and absolute entropy calculated for $Sc(OH)_2^+$, CH_3OScOH^+, $Sc(OCH_3)_2^+$, $CH_3OScOCH_2CH_3^+$, H_2O, CH_3OH, and CH_3CH_2OH at the LMP2 level of theory. Because the LMP2 level of theory is size consistent, ΔH can be calculated as the difference of the electronic energies of the products and electronic energies of the reactants (with zero-point energies taken into account). The calculated ΔH_{298}, ΔS_{298}, and ΔG_{298} for reactions (28)–(30) are given in Table 3.

In order to estimate the accuracy of these calculations, we have compared, where possible, the calculated values of $H_{298} - H_0$ and $\bar{S}_{298}$ with the experimentally known values (see Table 2). For H_2O, CH_3OH, and CH_3CH_2OH the calculated values of $H_{298} - H_0$ agree very well with the experimental values, although the agreement worsens for the larger species. The calculated values of $\bar{S}_{298}$ for H_2O,

Table 2
Calculated total energies, zero-point energies (ZPE), 0–298 K enthalpy corrections ($H_{298} - H_0$) and absolute entropies[a]

Species	Total energy (Hartree)	ZPE (kcal mol^{-1})	$H_{298} - H_0$ (kcal mol^{-1})	$\bar{S}_{298}$ (cal mol^{-1} K^{-1})
H_2O	−76.19902	13.4	2.3 (2.4)	45.1 (45.1)
CH_3OH	−115.35021	33.0	2.6 (2.7)	56.7 (57.3)
CH_3CH_2OH	−154.52122	51.5	3.2 (3.4)	64.1 (67.5)
$Sc(OH)_2^+$	−152.77798	15.6	3.6	67.2
CH_3OScOH^+	−191.93894	34.5	4.6	77.7
$Sc(OCH_3)_2^+$	−231.09899	53.0	5.9	88.1
$CH_3OScOCH_2CH_3^+$	−270.26630	71.2	6.3	94.6

[a] Values shown in parentheses are experimental values [25].

Table 3
Calculated ΔH_{298}, ΔS_{298}, and ΔG_{298} for reactions (28)–(30)

Reaction	ΔH_{298} (kcal mol^{-1})	ΔG_{298} (kcal mol^{-1})[a]	ΔS_{298} (cal mol^{-1} K^{-1})[b]
$Sc(OH)_2^+ + CH_3OH \rightleftharpoons CH_3OScOH^+ + H_2O$	−5.9	−5.6 (−2.6)	−1.1 (0.0)
$CH_3OScOH^+ + CH_3OH \rightleftharpoons Sc(OCH_3)_2^+ + H_2O$	−5.7	−5.3 (−2.6)	−1.1 (−2.8)
$Sc(OCH_3)_2^+ + CH_3CH_2OH \rightleftharpoons CH_3OScOCH_2CH_3^+ + CH_3OH$	+3.3	+3.5 (+0.4)	−0.9 (+1.4)

[a] Values in parentheses are experimentally measured values of ΔG_{298} from this work.
[b] Values in parentheses are the values for ΔS_{298} predicted by Eq. (33).

CH_3OH, and CH_3CH_2OH are also in good agreement with the experimental values, though again the agreement worsens as the size of the species increases. It appears that the LMP2 level of theory systematically underestimates the values of both $H_{298} - H_0$ and $\bar{S}_{298}$, with the error increasing as the size of the species increases. For ethanol, the calculated $\bar{S}_{298}$ is in error by about 3 cal mol^{-1} K^{-1}, so we estimate that our calculated $\bar{S}_{298}$ values could be low by as much as 5–7 cal mol^{-1} K^{-1} for $CH_3OScOCH_2CH_3^+$, the largest species for which we performed calculations. The error in our calculated ΔS_{298} values for reactions (28)–(30) should be less than this, but because the systematic error increases with size, we estimate that uncertainty in our calculated ΔS_{298} values could be as large as ± 2 cal mol^{-1} K^{-1}. We also compared our calculated values of ΔG_{298} for reactions (28)–(30) with the experimental values derived for reactions (6), (7), and (11) (see Table 3). In each case the calculated value differs from the experimental value by about 3 kcal mol^{-1}. The errors do not appear to be systematic, so the uncertainty in our calculated ΔG_{298} values are estimated to be at least ± 3 kcal mol^{-1}.

5. Discussion

5.1. Overview

In this study we were able to observe sigma-bond metathesis reactions of $Sc(OCD_3)_2^+$ with water, ethanol, and 1-propanol. This reactivity is analogous to the reactions of $Sc(CD_3)_2^+$ and $CH_3ScCH_2CH_3^+$ with small alkanes [10–12]. However, with $Sc(OCD_3)_2^+$ and water, ethanol, or 1-propanol, we succeeded in establishing ligand exchange equilibria via sigma-bond metathesis [reactions (6), (7), (11), (12), and (22)] and measured the equilibrium constants (see Table 1) for these processes. These metathesis reactions could proceed via an oxidative addition/reductive elimination pathway or via a four-center intermediate. Because Sc^+ has only two valence electrons

Table 4
Gas phase bond energies at 298 K for chemical species relevant to this article

Species	D^o_{298} (kcal mol^{-1})[a,b]
HO–H	119 (1)
CH_3O–H	104.4 (1)
CD_3O–H	104.2 (1)[c]
CH_3CH_2O–H	104.2 (1)
$CH_3CH_2CH_2O$–H	103.4 (1)
Sc^+–OH	120.4 (2.1)[d], 118.8[e]
$HOSc^+$–OH	126.9 (2.1)[f]
HSc^+–H	59 (4)[g]
HSc^+–D	60 (4)[h]
Sc^+–O═CD_2	39 (5)[i]
Sc^+–O═$CHCH_3$	43 (5)[i]
Sc^+–(CD_3OH)	30 (5)[i]
Sc^+–(CH_3CH_2OH)	35 (5)[i]

[a] Uncertainties are in parentheses.
[b] Unless otherwise noted, all values come from [20].
[c] Calculated from values in [21].
[d] [28]. The value here has been corrected by 1.2 kcal mol^{-1} to convert it from D^o_0 to D^o_{298}.
[e] Theoretical value, [29]. The value here has been corrected by 1.2 kcal mol^{-1} to convert it from D^o_0 to D^o_{298}.
[f] Theoretical value (corrected by 1.2 kcal mol^{-1} to convert it from D^o_0 to D^o_{298} is 125.3 kcal mol^{-1} [29]. Since theoretical value for Sc^+–OH bond energy was underestimated by 1.6 kcal mol^{-1}, we have adjusted the theoretical bond energy for $HOSc^+$–OH upward by the same amount.
[g] [30].
[h] This value has been corrected by 1 kcal mol^{-1} to account for the change in D^o_{298} upon substituting D for H.
[i] See discussion in text.

Table 5
Bond energies of Sc^+–alkoxide bonds relative to Sc^+–OCD_3[a]

Species (CD_3OSc^+–OR)	$D^o_{298}(CD_3OSc^+–OR)–D^o_{298}(CD_3OSc^+–OCD_3)$[b] (kcal mol^{-1})
CD_3OSc^+–OH	+11.9[c]
CD_3OSc^+–OCD_3	0.0
CD_3OSc^+–OCH_2CH_3	−0.1
CD_3OSc^+–$OCH_2CH_2CH_3$	−1.4

[a] The uncertainty in these values is estimated to be ±0.5 kcal mol^{-1}.
[b] Calculated from Eq. (34).
[c] Calculated assuming $D^o_{298}(CD_3OSc^+–OH) = D^o_{298}(HOSc^+–OH)$.

with which to form strong sigma bonds [26,27], we favor a four-center mechanism for these metathesis reactions [13] (as shown in Scheme 1 for the reaction of $Sc(CD_3)_2^+$ with *n*-butane).

5.2. Calculation of bond energies

As Bryndza et al. [1] have shown, equilibrium data from sigma-bond metathesis reactions can be used to determine the relative metal–ligand bond strengths for a series of complexes. To illustrate, consider the general sigma-bond metathesis process shown in reaction (31), where R = H or alkyl. Eq. (32) relates K to ΔH

$$Sc(OCD_3)_2^+ + ROH \rightleftharpoons CD_3OSc^+–OR + CD_3OH \quad (31)$$

$$\Delta H = -RT \ln K + T\Delta S \quad (32)$$

Since our study was conducted at a single temperature, we are unable to experimentally measure ΔS.

Table 6
Gas phase Sc^+–oxygen bond energies at 298 K[a]

Species	D^o_{298} (kcal mol^{-1})
$HOSc^+$–OH	126.9 (2.1)[b]
$HOSc^+$–OCD_3	115.0
CD_3OSc^+–OCD_3	115.0
CD_3OSc^+–OCH_2CH_3	114.9
CD_3OSc^+–$OCH_2CH_2CH_3$	113.6
$CH_3CH_2OSc^+$–OCH_2CH_3	114.7

[a] The uncertainty in these values is estimated to be ± 2 kcal mol^{-1}.
[b] See Table 4.

Table 7
Gas phase heats of formation at 298 K for chemical species relevant to this article

Species	$\Delta H^o_{f,298}$ (kcal mol^{-1})[a,b]
H	52.1 (0.1)
D	53.0 (0.1)
OCD_3	1.0 (1)[c]
OCH_2CH_3	−4.1 (0.1)[d]
O═CD_2	−27.5 (1)[e]
O═$CHCH_3$	−39.6 (0.1)

[a] Uncertainties are in parentheses.
[b] Unless otherwise noted, all values come from [34].
[c] Calculated from values in [21].
[d] [20].
[e] [35].

Theoretical calculations were used to estimate ΔS_{298} for reactions (28)–(30) (see Table 3), but the large size of $Sc(OCH_2CH_3)_2^+$ and $CD_3OScOCH_2CH_2CH_3^+$ made it impractical to perform ab initio calculations on them. However, vibrational contributions to ΔS are likely to be small for the metathesis reaction (31), and the main rotational contribution to ΔS will arise from symmetry numbers. Therefore, we can estimate ΔS for reactions (12) and (22) using Eq. (33),

$$\Delta S \approx R \ln \left[\prod_i \sigma_{i,\text{reactants}} / \prod_i \sigma_{i,\text{products}} \right] \quad (33)$$

where σ_i is the symmetry number of the ith species. The values of ΔS_{298} for reactions (28)–(30) predicted using Eq. (33) are also given in Table 3. Comparison with the LMP2 values of ΔS_{298} indicate that for metathesis processes, such as reaction (31), the entropies calculated from Eq. (33) are accurate to within ± 2.5 cal mol^{-1} K^{-1}. Because the error in our LMP2 values for ΔS_{298} is estimated to be ± 2 cal mol^{-1} K^{-1}, our estimates of ΔS for reactions (12) and (22) calculated from Eq. (33) appear to be reasonably accurate [31].

Once ΔH for reaction (31) is known, we can then calculate the *relative* bond strength between CD_3OSc^+–OCD_3 and CD_3OSc^+–OR with Eq. (34)

$$D^o(CD_3OSc^+–OR) - D^o(CD_3OSc^+–OCD_3) = D^o(RO–H) - D^o(CD_3O–H)\Delta H \quad (34)$$

If one R′OSc$^+$–OR bond strength is known from other experimental methods, then we can use appropriate equilibrium measurements to determine the *absolute* bond strengths of other Sc$^+$–alkoxide bonds. In fact, values for the Sc$^+$–OH and HOSc$^+$–OH bond energies are known (see Table 4). Therefore, using the method just outlined, we have determined the bond strengths for Sc$^+$–OR bonds where R = methyl, ethyl, and *n*-propyl. Bond strengths relevant to this work are given in Table 4, and the derived relative and absolute Sc$^+$–OR bond strengths are presented in Tables 5 and 6, respectively.

We should note that our experimental results are consistent with recent calculations by Bauschlicher and Partridge [29]. They find that the HOSc$^+$–OH bond is 8.8 ± 0.5 kcal mol^{-1} stronger than the HOSc$^+$–OCH$_3$ bond. They also note that the difference is likely underestimated by 1–2 kcal mol^{-1}, implying that the HOSc$^+$–OH bond is actually about 10.5 kcal mol^{-1} stronger than the HOSc$^+$–OCH$_3$ bond. In conjunction with their calculated bond strength for HOSc$^+$–OH of 126.9 kcal mol^{-1}, they calculate the HOSc$^+$–OCH$_3$ bond strength to be 116.4 ± 0.5 kcal mol^{-1}. This value is in good agreement with our experimental value of 115.0 ± 2.0 kcal mol^{-1} for the HOSc$^+$–OCD$_3$ bond strength, and provides additional evidence that subsequent solvation and elimination processes did not have a large effect on the measured equilibrium constants.

Examination of the bond energies in Tables 4 and 6 show that the trends in the Sc$^+$–OR and H–OR bond energies for R = H, methyl, ethyl, and *n*-propyl mirror each other closely. Similar behavior is seen when comparing Sc$^+$–R and H–R (R = alkyl) bond strengths [32]. Furthermore, since the trends in the Sc$^+$–OR and H–OR bond strengths correlate closely, we should be able to use H–OR (R = alkyl group larger than *n*-propyl) bond strengths to predict the corresponding Sc$^+$–OR bond strengths. Although the predictive value of such an approach has been previously demonstrated for liquid-phase ruthenium and platinum systems [1,33], this work provides additional evidence that this kind of correlation is generally valid with a wide range of organometallic compounds.

5.3. Elimination processes and reaction energetics

Although the main focus of this article is not concerned with the elimination of H_2 from solvated Sc$^+$-alkoxide species [reactions (19)–(21), (26), and (27)], we will make a few comments about these observed processes here. First, we note that in all these reactions no HD loss is observed. This indicates that the methoxy ligand does not participate in reactions (19) and (20). However, solvated Sc$^+$-alkoxide species containing either ethanol or the ethoxide ligand appear to readily dehydrogenate. Thus, it could be imagined that $CD_3OScOCH_2CH_3^+$ might isomerize to $CD_3OScH(O{=}CHCH_3)^+$.

To examine these points further, we have estimated the enthalpy of reactions (35) and (36). Relevant thermochemical values are shown in Tables 4, 6, and 7

$$CD_3OScOCD_3^+ \rightarrow CD_3OScD(O{=}CD_2)^+ \quad (35)$$

$$CD_3OScOCH_2CH_3^+ \rightarrow CD_3OScH(O{=}CHCH_3)^+ \quad (36)$$

Most of the necessary values were obtained from the literature. However, we used the values from this work for the Sc$^+$–OCD$_3$ and Sc$^+$–OCH$_2$CH$_3$ bond energies, and because the Sc$^+$–O=CD$_2$ and Sc$^+$–O=CHCH$_3$ bond energies are not known, we estimated them as follows. Magnera et al. found the Sc$^+$–OH$_2$ bond strength to be 31.4 kcal mol^{-1} [36], whereas Bauschlicher and Langhoff calculate a value of 34.5 kcal mol^{-1} [37]. This suggests that adducts between Sc$^+$ and oxygen-containing species have comparatively low bond energies. Further, in previous work by Halle et al. [38], the Co$^+$–O=CH$_2$ and Co$^+$–O=CHCH$_3$ bond energies were estimated to be 43 kcal mol^{-1} and 47 kcal mol^{-1}, respectively. Because Bauschlicher and Langhoff calculated that the Co$^+$–OH$_2$ bond strength is about 4 kcal mol^{-1} higher than the Sc$^+$–OH$_2$ bond strength [37], we estimate the Sc$^+$–O=CD$_2$ and Sc$^+$–O=CHCH$_3$ bond energies to be 39 kcal mol^{-1} and 43 kcal mol^{-1}, respectively. With these thermochemical values, we can calculate that for reaction (35), ΔH = + 40.5 kcal mol^{-1}, whereas for reaction 36 ΔH = +28.6

kcal mol^{-1}. Thus, it appears quite unlikely that any $CD_3OScD(O{=}CD_2)^+$ or $CD_3OScH(O{=}CHCH_3)^+$ is being generated in our experiments.

5.4. Comparison of theoretical results with experimental observations

One interesting feature in our theoretically determined lowest energy geometries for $Sc(OH)_2^+$, CD_3OScOH^+, $Sc(OCD_3)_2^+$, and $CD_3OScOCH_2CH_3^+$ is the large Sc^+–O–C bond angles ($\approx$ 165°, see Fig. 11) that are found. Bauschlicher and Partridge obtained similar results from their optimization of the $Sc(OH)_2^+$ geometry [29]. These large Sc^+–O–C bond angles suggest that strong dative interactions between Sc^+ and each oxygen atom are occurring in all these ions [39]. The calculated O–Sc^+–O bond angles of 116°–122° in these ions (see Fig. 11) are also indicative of significant dative interactions. We should note that such dative bonding has been observed previously with Sc^+–OH. Tilson and Harrison found that in the ground state Sc^+–OH has a linear geometry and a triple bond between Sc^+ and OH [40]. Also, previous work by Clemmer et al. [28] determined that $D_0^o(Sc^+–OH)$ = 119 kcal mol^{-1}, which is much greater than the $Sc^+–CH_3$ bond energy of 59 kcal mol^{-1} [30]. This enhanced bond strength for Sc^+–OH was attributed to the ability of the OH group to donate its two lone pairs of electrons to Sc^+ in a dative interaction.

However, atomic charges calculated from Mulliken populations indicate that Sc carries a net charge of about + 1.8 in $Sc(OH)_2^+$, CD_3OScOH^+, $Sc(OCD_3)_2^+$, and $CD_3OScOCH_2CH_3^+$ (varying from 1.84 in $Sc(OH)_2^+$ to 1.76 in $CD_3OScOCH_2CH_3^+$, with the net charge decreasing as larger alkoxide groups are added). This indicates a significant electrostatic contribution to the bonding. Thus our present results indicate that both ionic and dative interactions contribute significantly to the bonding between Sc^+ and each oxygen atom in diligated species. It also appears that both ligands can participate equally in dative interactions.

Acknowledgements

This work was supported by the National Science Foundation under Grant CHE-9108318, by a grant from AMOCO, and by the Office of Naval Research. We also wish to thank the Beckman Foundation and Institute for continuing support of the FT-ICR research facility and the Beckman Institute Materials and Process Simulations Center (supported by DOE-BCTR and the National Science Foundation under Grant CHE-9522179) for supporting our theoretical calculations. Francesco Faglioni and Jason K. Perry gave especially helpful advice concerning the theoretical calculations in this work.

References

[1] H.E. Bryndza, L.K. Fong, R.A. Paciello, W. Tam, J.E. Bercaw, J. Am. Chem. Soc. 109 (1997) 1444.
[2] J.S. Uppal, D.E. Douglas, R.H. Staley, J. Am. Chem. Soc. 103 (1981) 508.
[3] C.S. Christ, J.R. Eyler, D.E. Richardson, J. Am. Chem. Soc. 110 (1988) 4038.
[4] M.J. Wax, J.M. Stryker, J.M. Buchanan, C.A. Kovac, R.G. Bergman, J. Am. Chem. Soc. 106 (1984) 1121.
[5] J.M. Buchanan, J.M. Stryker, R.G. Bergman, J. Am. Chem. Soc. 108 (1986) 1537.
[6] G. Jeske, H. Lauke, H. Mauermann, H. Schumann, T.J. Marks, J. Am. Chem. Soc. 107 (1985) 8111.
[7] P.L. Watson, J. Am. Chem. Soc. 105 (1983) 6491.
[8] M.E. Thompson, S.M. Baxter, A.R. Bulls, B.J. Burger, M.C. Nolan, B.D. Santarsiero, W.P. Schaefer, J.E. Bercaw, J. Am. Chem. Soc. 109 (1987) 203.
[9] Y. Huang, Y.D. Hill, M. Sodupe, C.W. Bauschlicher Jr., B.S. Freiser, J. Am. Chem. Soc. 114 (1992) 9106.
[10] K.C. Crellin, J.L. Beauchamp, S. Geribaldi, M. Decouzon, Organometallics 15 (1996) 5368.
[11] K.C. Crellin, S. Geribaldi, M. Widmer, J.L. Beauchamp, Organometallics 14 (1995) 4366.
[12] K.C. Crellin, S. Geribaldi, J.L. Beauchamp, Organometallics 13 (1994) 3733.
[13] M.L. Steigerwald, W.A. Goddard III, J. Am. Chem. Soc. 106 (1984) 308.
[14] M. Azzaro, S. Breton, M. Decouzon, S. Geribaldi, Int. J. Mass Spectrom. Ion Processes 128 (1993) 1.
[15] A.G. Marshall, Acc. Chem. Res. 18 (1985) 316.
[16] M.B. Comisarow, Anal. Chim. Acta 178 (1985) 1.
[17] L.R. Anders, J.L. Beauchamp, R.C. Dunbar, J.D. Baldeschwieler, J. Chem. Phys. 45 (1966) 1062.
[18] M.B. Comisarow, A.G. Marshall, Chem. Phys. Lett. 26 (1974) 489.

[19] J.H. Espenson, Chemical Kinetics and Reaction Mechanisms, McGraw-Hill, New York, 1981.
[20] D.F. McMillen, D.M. Golden, Ann. Rev. Phys. Chem. 33 (1982) 493.
[21] S.E. Barlow, T.T. Dang, V.M. Bierbaum, J. Am. Chem. Soc. 112 (1990) 6832.
[22] M.N. Ringnalda, J.-M. Langlois, B.H. Greeley, R.B. Murphy, T.V. Russo, C. Cortis, R.P. Muller, B. Marten, R.B. Donnelly Jr., D.T. Mainz, J.R. Wright, W.T. Pollard, Y. Cao, Y. Won, G.H. Miller, W.A. Goddard III, R.A. Friesner, PS-GVB, v.2.2, Schrödinger Inc., 1995.
[23] Specifically, we used the LAV3P* ECP basis set. P.J. Hay, W.R. Wadt, J. Chem. Phys. 82 (1985) 270.
[24] In the interests of saving space, the complete listing of bond lengths and bond angles for these structures are not presented in this article. However, we have tabulated these parameters. If desired, the files containing these parameters can be obtained from the authors upon request.
[25] D.D. Wagman, W.H. Evans, V.B. Parker, I. Halow, S.M. Baily, R.H. Schumm, Selected Values of Chemical Thermodynamic Properties, National Bureau of Standards Technical Note 270-3, United States Government Printing Office, Washington, DC, 1968.
[26] M.A. Tolbert, J.L. Beauchamp, J. Am. Chem. Soc. 106 (1984) 8117.
[27] J.L. Beauchamp, P.A.M. van Koppen, in Energetics of Organometallic Species, J.A.M. Simoes (Ed.), Kluwer Academic, Dordrecht, 1992.
[28] D.E. Clemmer, N. Aristov, P.B. Armentrout, J. Phys. Chem. 97 (1993) 544.
[29] C.W. Bauschlicher Jr., H. Partridge, personal communication.
[30] P.B. Armentrout, R. Georgiadis, Polyhedron 7 (1988) 1573.
[31] The quality of our calculations can also be gauged by comparing the theoretically calculated values of ΔG_{298} with our experimental values. For reactions (28)–(30), the calculated value of ΔG_{298} for each reaction was within 3.1 kcal mol^{-1} of the experimental value. Furthermore, the calculated values of ΔG_{298} for reactions (28) and (29) were within 0.3 kcal mol^{-1} of each other, in excellent agreement with our experimental results. Thus the LMP2 level of theory appears to perform reasonably well at calculating the thermodynamic values associated with these metathesis reactions.
[32] J.K. Perry, W.A. Goddard III, J. Am. Chem. Soc. 116 (1994) 5013.
[33] H.E. Bryndza, W. Tam, Chem. Rev. 88 (1988) 1163.
[34] S.G. Lias, J.E. Bartmess, J.F. Liebman, J.L. Holmes, R.D. Levin, W.G. Mallard, J. Phys. Chem. Ref. Data 17 (1988) (Suppl.).
[35] M. Frenkel, K.N. Marsh, R.C. Wilhoit, G.J. Kabo, G.N. Roganov, Thermodynamics of Organic Compounds in the Gas Phase, Vol. I, Thermodynamics Research Center, College Station, Texas, 1994.
[36] T.F. Magnera, D.E. David, J. Michl, J. Am. Chem. Soc. 111 (1989) 4100.
[37] C.W. Bauschlicher Jr., S.R. Langhoff, Int. Rev. Phys. Chem. 9 (1990) 149.
[38] L.F. Halle, W.E. Crowe, P.B. Armentrout, J.L. Beauchamp, Organometallics 3 (1984) 1694.
[39] Dative interactions increase bond angles because the lone pairs of electrons formally become bonding pairs. The loss of a lone pair character and the gain of a pi bonding character lead to increased bond angles.
[40] J.L. Tilson, J.F. Harrison, J. Chem. Phys. 95 (1991) 5097.